Minor hysteresis loops and harmonic generation calculations in a generalized critical-state model

P. Chaddah, S. B. Roy, and Shailendra Kumar
Low Temperature Physics Group, Centre for Advanced Technology, Indore 452 013, India

K. V. Bhagwat
Solid State Physics Division, Bhabha Atomic Research Centre, Bombay 400 085, India

(Received 24 March 1992)

We present analytic calculations of minor hysteresis loops obtained when a sample is subjected to a time-varying field $B(t)=B_{dc}+B_{ac}\cos\omega t$. We enumerate eight classes of minor hysteresis loops, and calculations are done within the critical-state model but for an arbitrary field dependence of the critical current density $J_c(B)$. The sample shapes considered are the zero-demagnetization factor cases of a circular cylinder, and of a slab, in a longitudinal field. Harmonic components of the magnetization (M_n) are numerically obtained for various forms of $J_c(B)$. Our results bring out the importance of the sample shape used in the calculation and also point out the features in M_n vs B_{dc} that clearly reflect the details of the field dependence in $J_c(B)$.

I. INTRODUCTION

The critical-state model has been extensively used to calculate the magnetization hysteresis curves of high-T_c superconductors (HTSC). While Bean's initial calculation[1] assumed that the critical current density (J_c) is independent of field, many special forms of $J_c(B)$ have been used in the last few years to explain the magnetization data on the HTSC. Recent work,[2-7] measuring the harmonic generation in HTSC pellets subjected to a time-varying field $B(t)=B_{dc}+B_{ac}\cos\omega t$, has focused attention on minor hysteresis loops.[8] While the minor hysteresis loop can also be measured with any magnetization measurement setup, the harmonics of the magnetization are more commonly measured.[2-7] As was emphasized by Ji *et al.*,[2] the finite magnitude of even harmonics for $B_{dc}\neq 0$ is a clear qualitative signature that $J_c(B)$ has a field dependence. There has thus been a reasonable expectation that the dependence of the harmonic magnitude (M_n) on B_{dc} and B_{ac} could provide a detailed check on the form of $J_c(B)$. A prerequisite to calculating M_n is the calculation of the minor hysteresis loop, and we shall do this here for arbitrary $J_c(B)$. The complex harmonics, and thus their magnitude M_n, are then obtained easily by a numerical Fourier transform.

LeBlanc, Fillion, and Lorrain[9] had calculated minor hysteresis loops for various specific forms of $J_c(B)$, and had used these to calculate hysteresis losses in the presence of dc fields. They had considered the sample geometries of a slab and of a circular cylinder in longitudinal fields. Subsequent to the measurements of harmonic generation in the HTSC, calculations of the minor hysteresis loops and harmonic generation have been performed for the sample geometry of a slab in a longitudinal field with $J_c(B)$ assumed to vary as $[\alpha/|B|]$,[2,3,7] or as $[J_c(0)/(1+|B|/B_0)]$,[4-6] or as $[J_c(0)/(1+|B|/B_0)^q]$.[5] Recently, Wahid and Jaggi[10] have calculated the minor hysteresis loops for the last form of $J_c(B)$ but for the sample geometry of a circular cylinder in a longitudinal field. It is to be noted that a comparison between calculations of harmonic generation for the two sample geometries will bring out geometrical artifacts, especially since neither shape is a realistic shape for typical HTSC samples. Further, calculations have not been performed for some commonly used forms of $J_c(B)$ such as the exponential form[11] $[J_c(0)\exp(-|B|/B_0]$, or the power-law form[12] $[\alpha/|B|^q]$. Not only does this leave gaps for piecemeal calculations using a particular form of $J_c(B)$, it also requires detailed calculations before a new form of $J_c(B)$ can be tested.

Recently Bhagwat and Chaddah[13] solved analytically the magnetization hysteresis curve for a cylinder of elliptic cross section in a longitudinal field. The formalism of their analytic calculation was developed for an arbitrary form of $J_c(B)$. We shall follow their scheme and obtain analytic results for the minor hysteresis loops for arbitrary $J_c(B)$. This formalism requires defining a canonical field variable[13,14]

$$h=\int d|B|/\mu_0 J_c(|B|) \tag{1}$$

and the integral can be analytically evaluated for all forms of $J_c(B)$ known to the present authors. We must mention here that the present calculation, like those cited earlier,[2-7,9] is for a homogeneous hard superconductor with $H_{c1}=0$, and its relevance to harmonic generation in sintered HTSC pellets will be justified only in Sec. V.

In Sec. II, we present our formalism, and in Sec. III the details of calculation of minor hysteresis loops. Both slab and circular cylinder geometries are considered. In Sec. IV, we present the calculation of harmonics. The effect of sample geometry and the change of features in M_n vs B_{dc} as one changes the form of $J_c(B)$ are brought out. In Sec. V, we discuss the relevance of our calculations to harmonic generation measurements in HTSC pellets.

II. FORMALISM OF THE CALCULATION

A. The field profile

The first step towards calculating the magnetization is to calculate the flux profile $B(r)$ within the sample. Magnetization is then obtained as $\mu_0\langle M\rangle = -B_a + (1/V)\int B(r)d\mathbf{r}$, where B_a $(=\mu_0 H_a)$ is the externally applied field, $\langle M\rangle$ is the spatial average of $M(\mathbf{r})$ over the sample volume, and the integral is over the sample volume. The profile $B(\mathbf{r})$ depends on B_a, on the magnetic history before B_a was applied, and also on the form of $J_c(B)$. The method of calculating the flux profile (for isothermal changes in B_a) within the critical-state model is well documented in recent literature (see, e.g., Ref. 13, and references therein). As noted by Wahid and Jaggi,[10] the algebraic manipulations required for calculating the minor hysteresis loops become quite clumsy. In the formalism presented below we use the canonical field variable $h(B)=\int d|B|/\mu_0 J_c(|B|)$ and the "clumsiness of the algebra"[10] is reduced to a minimum because we consider the dependence of $\langle M\rangle$ on B_a and on magnetic history in one step, and the relation between h and B [which involves $J_c(B)$] is treated separately. Further, before considering any new form of $J_c(B)$, only the relation between h and B has to be worked out afresh. We note here that h depends only on $|B|$ and decreases to $h(B=0)\equiv h_0$ as B decreases to zero. As B becomes negative and decreases further, h again starts increasing above h_0. We also note that h has the dimensions of length.

We consider a circular cylinder of radius R subjected to a large negative field, which is then raised isothermally

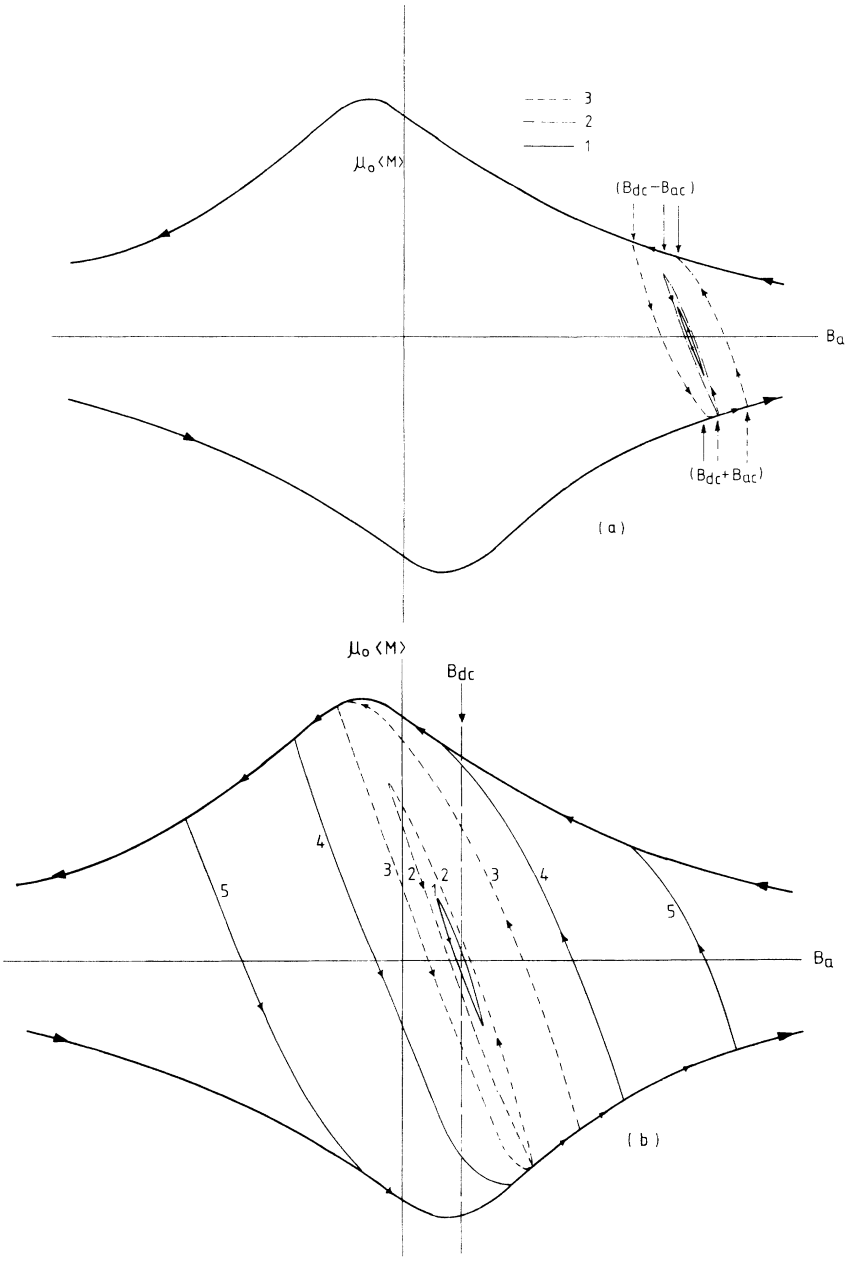

FIG. 1. (a) A schematic showing minor hysteresis loops for $B_{dc} > B_{ac}$. The sample is field cooled in B_{dc}, and then the field is raised to $B_{dc}+B_{ac}$. The minor loops are obtained when the field is now lowered to $B_{dc}-B_{ac}$, and raised back to $B_{dc}+B_{ac}$. The thick curves are the envelope hysteresis curves corresponding to $B_{dc}=0$ and $B_{ac}=\infty$. Three classes of minor hysteresis loops shown differ qualitatively in their contact and overlap with the envelope curves. (b) Same as (a) except that $B_{dc} < B_{ac}$. Here five classes of minor hysteresis loops are obtained. (c) Minor loop of class 1 of (a) is shown for different sample histories. See text for details.

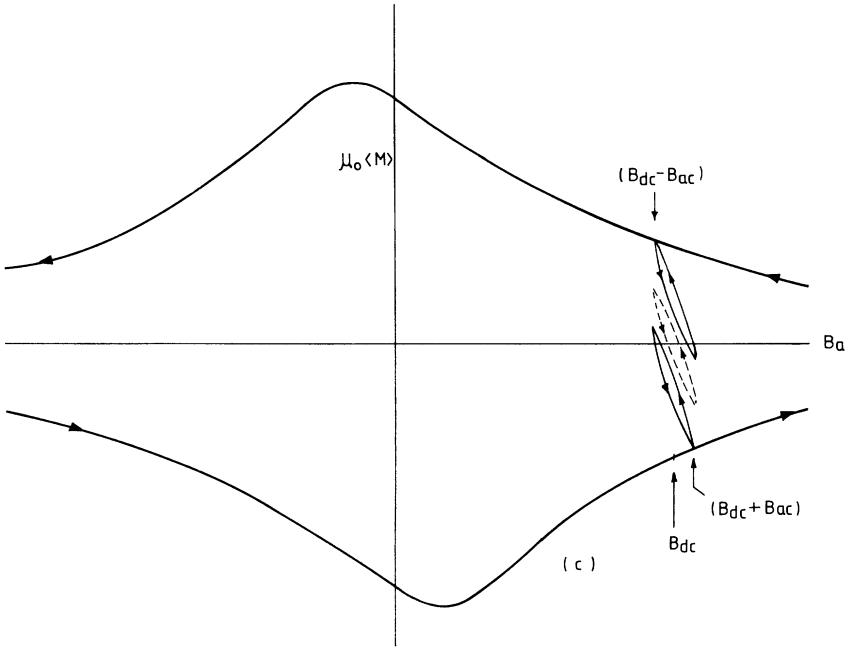

FIG. 1. (*Continued*).

to some positive B_a. $B(r)$ then decreases monotonically from $r=R$ to 0, and is dictated by $dB(r)/dr=\mu_0 J_c[B(r)]$. If $B(r)$ does not become negative for any r, then $h(r)$ also decreases inwards monotonically as dictated by $dh(r)/dr=1$, with the boundary conditions $h(R)=h(B_a)$ and $h(0)=h(B_a)-R$. [If, however, $h(B_a)<h_0+R$, then $B(r)$ changes sign at[13] $r_0=R-h(B_a)+h_0$ and $dh(r)/dr=-1$ for $r<r_0$.] If the applied field is now lowered from B_a to B_m, $B(r)$ increases inwards for $r>r_1$ satisfying $2(R-r_1)=h(B_a)-h(B_m)$ and decreases inwards for $r<r_1$. When B_m is lowered below B_1 such that $h(B_1)=h(B_a)-2R$, $B(r)$ increases monotonically from $r=R$ to $r=0$. At that stage we have $dB(r)/dr=-\mu_0 J_c[B(r)]$ and $dh(r)/dr=-1$. [If, however, $h(B_a)<h_0+2R$, then $B(r)$ will become monotonic only for B_m lower than a negative field B_1 satisfying $h(B_1)+h(B_a)-2h_0>2R$.] The evolution of $B(r)$ and $h(r)$ as the applied field is varied is discussed in more detail in Ref. 13.

B. Classifying minor loops

When the applied field is cycled between $B_{dc}+B_{ac}$ and $B_{dc}-B_{ac}$ (we assume $B_{dc}>0$ without any loss of generality), the minor hysteresis loop falls into one of eight possible classes. To illustrate these experimentally distinguishable classes, we show in Fig. 1 schematic hysteresis loops with the assumption that $J_c(B)$ decreases as $|B|$ increases. The thick envelope curves are the hysteresis curves obtained when the applied field is cycled between $\pm B_{max}$ with $B_{max}\to\infty$. The magnetization lies on this envelope curve only when $B(r)$ varies monotonically from $r=0$ to R. The field increasing and decreasing cases have positive and negative dB/dr, respectively.

Out of these eight classes, three are obtained when $B_{dc}>B_{ac}$ and these are shown in Fig. 1(a). We assume that the sample was initially prepared by field cooling (where $M=0$ since $H_{c1}=0$) in B_{dc} and the field is isothermally raised to $B_{dc}+B_{ac}$, and then cycled between $B_{dc}+B_{ac}$ and $B_{dc}-B_{ac}$. For fixed B_{dc} the minor loop changes from form 1 to 3 as B_{ac} is raised. In form 1 the loop does not touch either envelope curve, and such a loop is observed when $h(B_{dc}+B_{ac})-h(B_{dc})<R$. In form 2 the minor loop has a contact point with only one (in this case the field-increasing) envelope curve, but does not touch the field-decreasing envelope curve. This loop is seen when $h(B_{dc}+B_{ac})-h(B_{dc})>R$, but $h(B_{dc}+B_{ac})-h(B_{dc}-B_{ac})<2R$. In form 3 the minor loop has a finite overlap with both envelope curves, and this is seen when $h(B_{dc}+B_{ac})-h(B_{dc}-B_{ac})>2R$. It is easy to see that a loop of form 1 will change successively to forms 2 and 3 if B_{dc} is raised with B_{ac} held fixed.

If $B_{dc}<B_{ac}$ then the minor hysteresis loop can belong to one of the five classes indicated in Fig. 1(b). Form 1, which does not touch either envelope hysteresis curve, is obtained when $h(B_{dc}+B_{ac})-h(B_{dc})<R$. Form 2, which touches only one (in this case the field-increasing) envelope, is obtained when $h(B_{dc}+B_{ac})-h(B_{dc})>R$, but $h(B_{dc}+B_{ac})+h(B_{dc}-B_{ac})-2h_0<2R$. Forms 3, 4, and 5 are obtained when $h(B_{dc}+B_{ac})+h(B_{dc}-B_{ac})-2h_0>2R$, and have finite overlap with both envelope curves. In form 3 the overlap occurs only after the minor loop crosses $B_a=0$ in either direction, and this is seen when $h(B_{dc}+B_{ac})-h_0<2R$. For form 4 we have $h(B_{dc}+B_{ac})-h_0>2R$, but $h(B_{dc}-B_{ac})-h_0<2R$. In this case the minor loop merges with the field-decreasing envelope curve before crossing $B_a=0$. Form 5 is obtained when $h(B_{dc}-B_{ac})-h_0>2R$, and the minor loop merges with either envelope curve before crossing $B_a=0$. This completes the enumeration of the

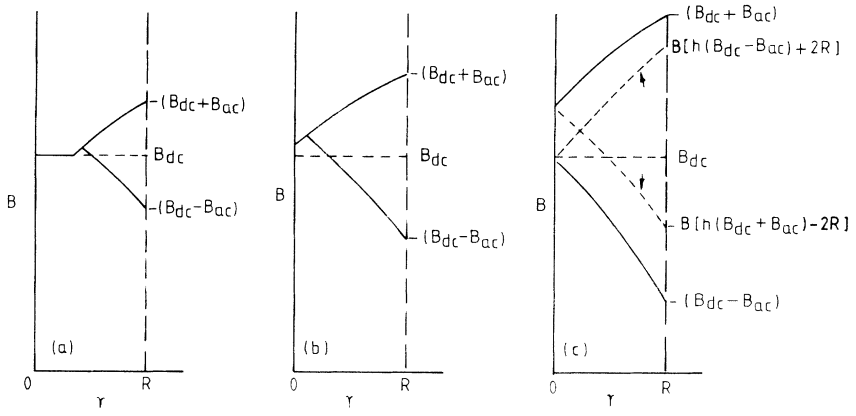

FIG. 2. We show schematic flux profiles for $B_{dc} > B_{ac}$, and (a), (b), and (c) correspond to minor loops 1, 2, and 3, of Fig. 1(a). The solid lines give the flux profiles at the two limiting values of applied field. The dashed line in (c) indicates $B(r)$ when $\langle M(B_a)\rangle$ starts overlapping with the envelope curve, and the arrow indicates a field-increasing or -decreasing case.

eight classes of minor hysteresis loops.

We wish to point out here that the initial state in which the sample is prepared affects the minor hysteresis loop only if the loop is of form 1 or 2 [for both signs of $(B_{dc}-B_{ac})$]. It is easy to show that even in these cases, changing the initial state only displaces the loop but does not affect its shape. For form 1 and $B_{dc} > B_{ac}$, we show this schematically in Fig. 1(c). We consider samples initially prepared in three different states: (i) subject to B_{dc} in the field-cooled (FC) state and then brought isothermally to $B_{dc}+B_{ac}$; (ii) to lie on the field-increasing envelope curve at $B_{dc}+B_{ac}$; and (iii) to lie on the field-decreasing envelope curve at $B_{dc}-B_{ac}$. Since the shapes of the three loops are identical, so are the harmonics. In view of the simplicity of analyzing HTSC pellets[15] when B_{dc} is applied before cooling, we shall calculate minor loops only for the FC case.

III. CALCULATION OF MAGNETIZATION

For obtaining the minor hysteresis loops we have to calculate the magnetization $\langle M(t)\rangle$ for values of B_a given by $B_a(t)=B_{dc}+B_{ac}\cos\omega t$. For a sample of volume V, the magnetization is given by

$$\mu_0\langle M(B_a)\rangle = -B_a + (1/V)\int B(r)\,d\mathbf{r}\ , \tag{2}$$

and the flux profile $B(r)$ depends on B_a, on B_{dc} and B_{ac}, and on whether the field was being raised or lowered to reach B_a. The dependence of $B(r)$ on $J_c(B)$ will become implicit and will get decoupled when we change the field parameter from B to $h(B)$. In Figs. 2 and 3 we show the schematic field profiles for $B_a=B_{dc}+B_{ac}$ and $B_a=B_{dc}-B_{ac}$ for the eight classes of minor loops indi-

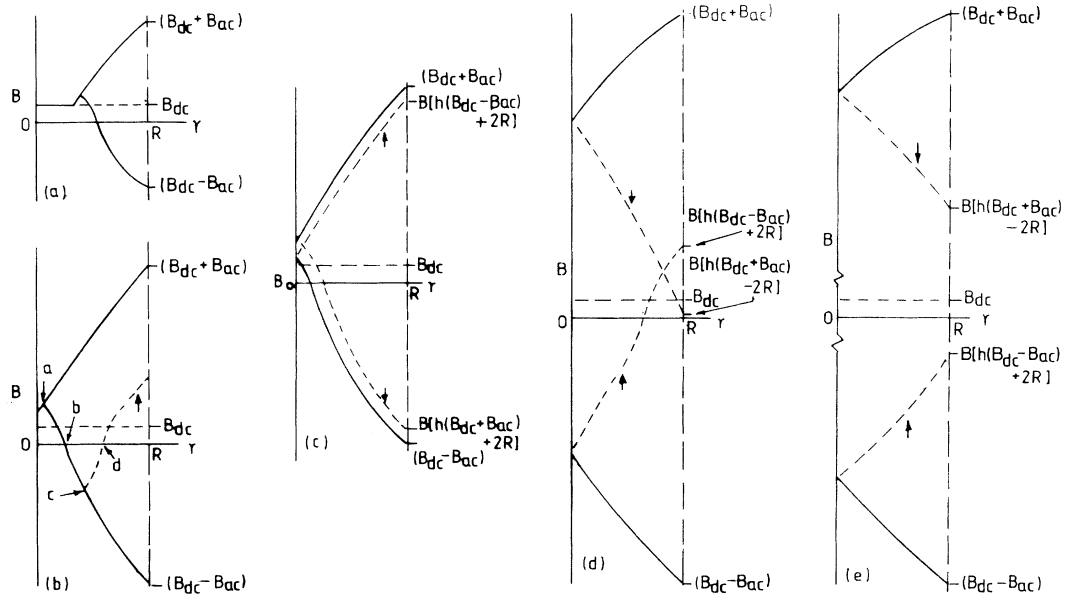

FIG. 3. Same as Fig. 2 except that $B_{dc} < B_{ac}$ and (a)–(e) correspond to forms 1–5 of Fig. 1(b). In (b) we also show $B(r)$ for an intermediate applied field for the field-increasing case. $h(B)$ changes its slope at the four points indicated.

cated in Fig. 1. For the four classes with finite overlap with the envelope curves, we also indicate the flux profiles for the applied field values where the overlap begins. For B_a values where $\langle M(B_a)\rangle$ is not on an envelope curve, $B(r)$ is not a monotonic function of r. Further, since $h(B)$ is a function of $|B|$, dh/dr also changes sign where $B(r)$ changes sign. In Fig. 3(b) we indicate a $B(r)$ profile for which dh/dr has the largest number of changes in sign for any field-cooled sample subjected to $B_{dc}+B_{ac}\cos\omega t$. $h(r)$ is increasing between 0 and a, decreasing to h_0 between a and b, increasing above h_0 between b and c, decreasing to h_0 between c and d, and increasing above h_0 between d and R.

Since we wish to evaluate $\langle M\rangle$ in terms of h, we note that both B and h are constant on a constant r surface. To change the integration variable from r to h in Eq. (2), we split the integral into n regions such that h varies monotonically in each region:

$$\mu_0\langle M\rangle = -B_a+\frac{1}{V}\left[\int_{r_0=0}^{r_1}B(r)d\mathbf{r}+\int_{r_1}^{r_2}B(r)d\mathbf{r}+\cdots+\int_{r_{m-1}}^{r_m=R}B(r)d\mathbf{r}\right]$$
$$= -B_a+\frac{1}{V}\sum_{i-1}^{m}\int_{h(r_i-1)}^{h(r_i)}B(h)g(h)dh\ , \tag{3}$$

where $h(r_i)=h[B(r_i)]$, and the largest value of m necessary is 5 as depicted in Fig. 3(b). We note that for a circular cylinder geometry $g(h)$ contains a term linear in h and a constant, while for a slab geometry $g(h)$ is independent of h. The integrals in Eq. (3) can then be written[13] in terms of

$$f_1(u,v)=\int_v^u B(h)dh\ ,$$
$$f_2(u,v)=\int_v^u B(h)hdh\ . \tag{4}$$

We thus find that $[\mu_0\langle M(B_a)\rangle+B_a]$ is written entirely in terms of f_1 and f_2. The only algebra left is to specify $h(r_i)=h[B(r_i)]$. This is done, following elementary but tedious algebra, in terms of the four quantities $h(B_{dc})$, $h(B_{dc}+B_{ac})$, $h(B_{dc}-B_{ac})$, and $h(B_a)$ for each of the eight types of minor hysteresis loops. $\langle M(t)\rangle$ is then known analytically for both circular cylinder and slab geometries for arbitrary B_{dc} and B_{ac}. The analytic expression for $(\mu_0\langle M(B_a)\rangle+B_a)$ in terms of f_1, f_2, $h(B_{dc})$, $h(B_{dc}+B_{ac})$, $h(B_{dc}-B_{ac})$, and $h(B_a)$ are not listed here to save space. The expressions for both these geometries are, however, available from the authors.

IV. RESULTS ON HARMONIC GENERATION

Once the minor hysteresis loops are known analytically it is a simple task to evaluate these at a large number of temporally equispaced applied fields $B_a(t)=B_{dc}+B_{ac}\cos\omega t$, and use a standard fast Fourier transform (FFT) routine to obtain the harmonics numerically. Both the real (M_n') and imaginary (M_n'') parts of the harmonics are obtained. Since the magnitude $M_n=\sqrt{M_n'^2+M_n''^2}$ is more commonly (and easily) measured, we shall concentrate on how M_n reflects the sample geometry and the details of $J_c(B)$. The calculation of M_n presented here shall be in units of (B^*/μ_0), and B_{dc} and B_{ac} shall be in units of $B^*=\mu_0 J_c(0)R$.

A. Sample-geometry effects

In zero dc field, M_3 is the first signature of nonlinearity and it has been studied in some detail. It has been argued[6] that $M_3\sim B_{ac}^2$ for J_c independent of B, and that a deviation from this implies that the field dependence of J_c is significant.

In Fig. 4(a), we plot M_3 vs B_{ac}^2 with Bean's[1] field independent J_c and $B_{dc}=0$. We note that the belief[2,6] that $M_3\sim B_{ac}^2$ for $B_{ac}<\mu_0 J_c R$ is valid only for the slab geometry. The dependence is slower for the cylinder geometry. In Fig. 4(b), we plot the same function but for an exponential $J_c(B)$. In this case M_3 vs B_{ac} shows a peak, and we note that even the position of the peak depends on the sample geometry used. In Fig. 4(c) we plot M_5 vs B_{dc}, for B_{ac} held fixed, for an exponential $J_c(B)$. We observe a clear difference between the results for the two geometries. The results presented in Fig. 4 bring out the importance of using an appropriate sample geometry in the calculation.

Using the fact that a sharp field dependence in $J_c(B)$ gives a peak in the hysteresis curve close to $B_a=0$, Ji *et al.*[2] have argued that M_5 is expected to show two minima between $B_{dc}=0$ and $B_{dc}=B_{ac}$. Our calculations predict that the extent of the minima, as measured by the peak-to-valley ratio, rises as B_{ac} is raised above B^*. These predictions will be compared with experimental observations in a separate paper.[16] We shall now discuss calculations for $B_{ac}\gg B^*$ when M_n vs B_{dc} shows strong minima.

B. Manifestation of details of $J_c(B)$

Amongst the various forms of $J_c(B)$ being used in literature we consider the exponential form $J_c(B)/J_c(0)=\exp(-|B|/B_0')$, and also the two-parameter form $J_c(B)/J_c(0)=(1+|B|/B_0)^{-\beta}$. As noted by Xu *et al.*,[17] the latter goes over into the exponential form with $B_0'=B_0/\beta$ as one takes the limit $B_0\to\infty$ with B_0/β held fixed. We accordingly present in Fig. 5 calculations of M_5 and M_6 for a cylinder for the two-parameter form of $J_c(B)$ with (i) $B_0=2$ and $\beta=1$; (ii) $B_0=3$ and $\beta=1.5$; (iii) $B_0=8$ and $\beta=4$. We also present results for the exponential form of $J_c(B)$ with $B_0'=2$. While the detailed shape of M_n vs B_{dc} does depend on the form of $J_c(B)$ used, the strongest effect is seen in the

peak-to-valley ratio of the maximum near $B_{dc}=0.7B_{ac}$. Since the field dependence increases for fixed B_0/β as B_0 is raised, we make the general statement that the sharpness of the structure in M_n vs B_{dc}, close to $B_{dc}=B_{ac}$, correlates directly with the sharpness of the field dependence of $J_c(B)$. This inference provides a guideline for harmonic measurements aimed at checking $J_c(B)$.

V. RELEVANCE TO MEASUREMENTS ON HTSC PELLETS

As mentioned in the Introduction, the calculation assumes that the hard superconductor is homogeneous and that its $H_{c1}=0$. For sintered HTSC pellets in low ac fields, the hysteresis and harmonic generation are from the intergrain region, and a vanishing H_{c1} is a reasonable approximation. The pellets are, however, highly inhomogeneous and the existence of contributions from both intergrain and intragrain regions to magnetization are well documented.[18–20] It has been brought out recently[15] that the dominant effect of the grains is to modify the effective field in the intergrain region. Since the magnetization of the grain depends on the history of the application of B_{dc}, so does the effective intergrain field and one sees a history effect in the harmonic generation from the inter-

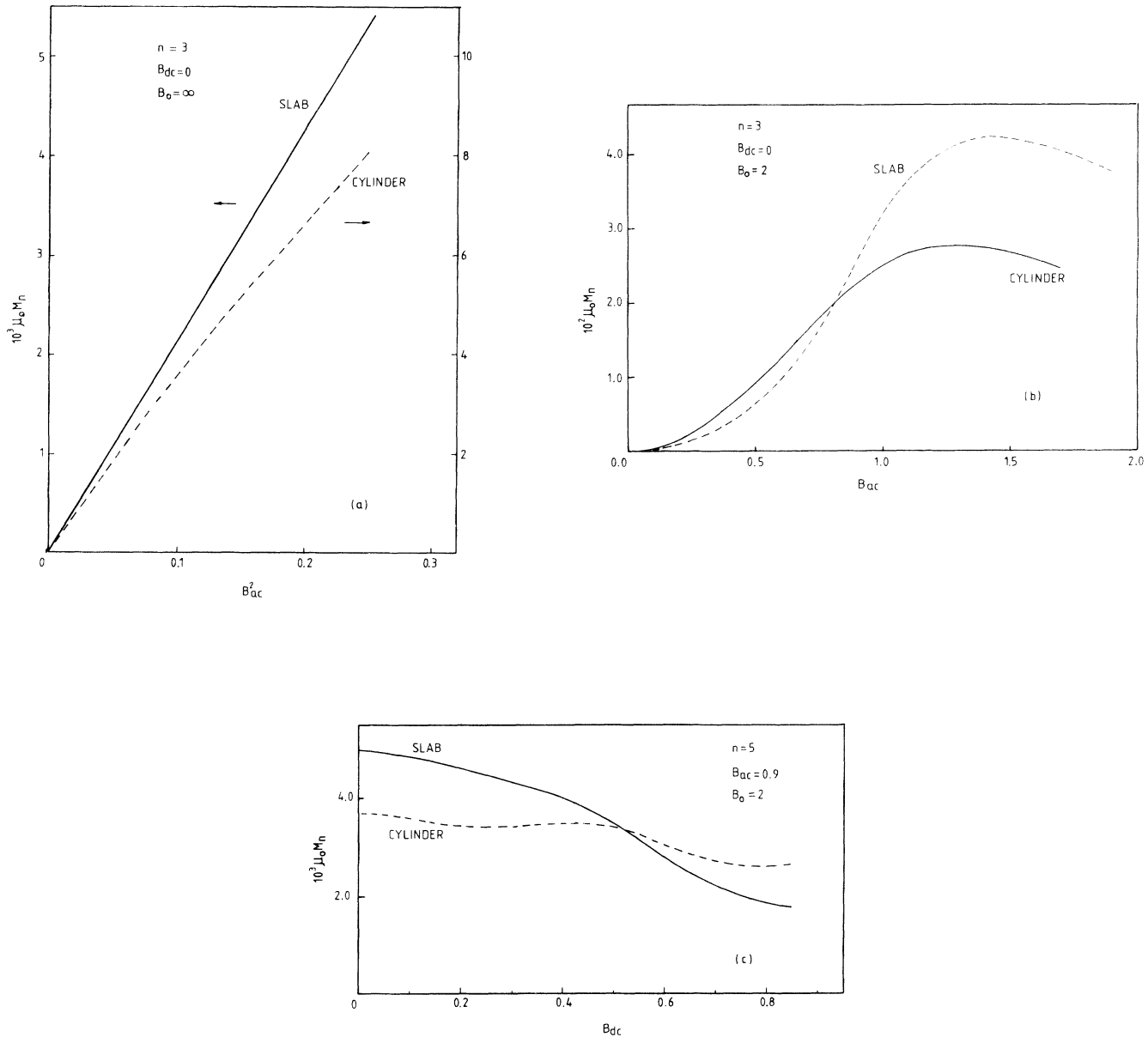

FIG. 4. (a) We plot M_3 vs B_{ac}^2 for $B_{dc}=0$ and field independent J_c. M_3 rises slower than B_{ac}^2 for the cylindrical case. We assume $B^*=\mu_0 J_c(0)R=1$ in all calculations of harmonics. B and $\mu_0 M_n$ are in units of B^*. (b) M_3 vs B_{ac} with $J_c(B)=J_c(0)\exp(-|B|/2)$. (c) We plot M_5 vs B_{dc} for the slab and cylinder geometries.

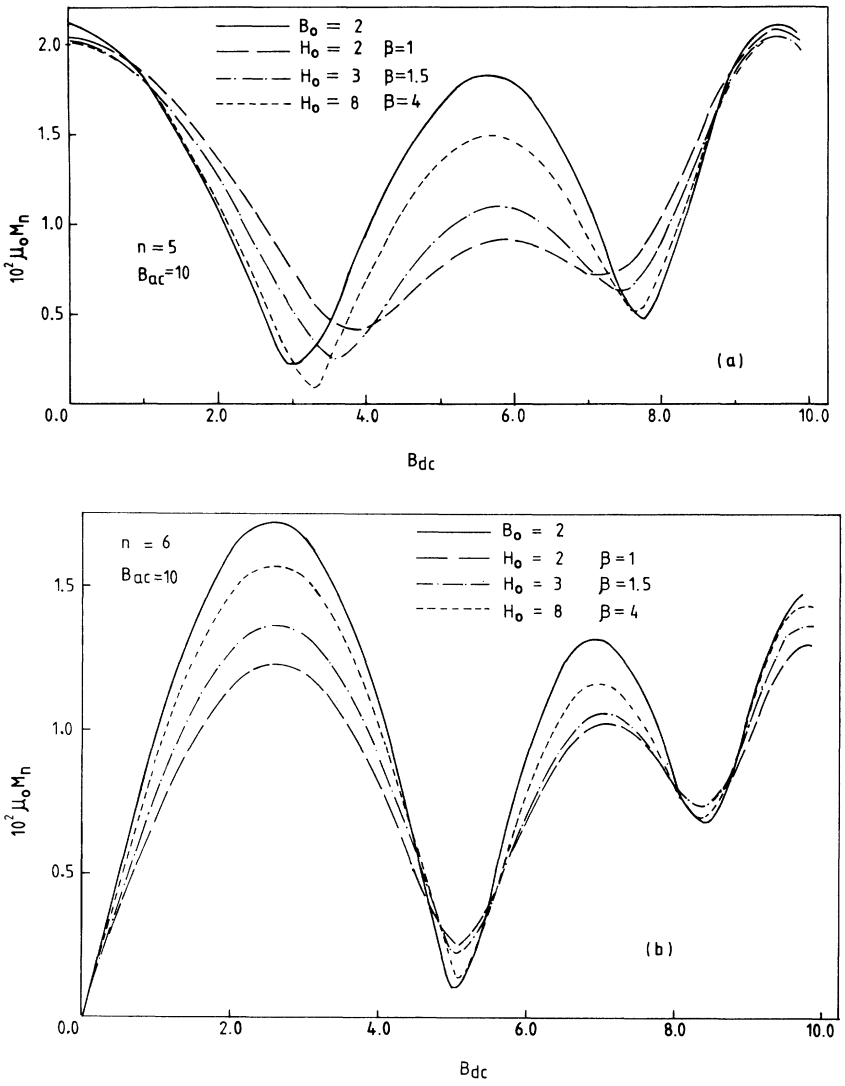

FIG. 5. (a) We plot M_5 vs B_{dc} for two forms of $J_c(B)$ viz $J_c(0)\exp(-|B|/B_0)$ and $J_c(0)[1+|B|/H_0]^{-\beta}$. The values of the parameters used are given. $\mu_0 M_5$ and B_{dc} are in units of B^*. (b) Same as (a) except that we plot M_6 vs B_{dc}.

grain region. This is contrary to what is expected from a homogeneous material where, as argued in Sec. II B, the harmonics are history independent. Since fine-filament NbTi/Cu wire shows evidence of being a two-component system in its hysteresis curves,[21] it is also expected to show history effects in harmonic generation. It was argued in Ref. 15 that such complicating effects of a two-component system would be minimized if all measurements are made with B_{dc} applied in the field-cooled mode. It is with such data on HTSC pellets that our calculations should be compared.

VI. CONCLUSION

In summary we have provided enumeration of experimentally distinguishable classes of minor hysteresis loops. Although the calculations are limited to shapes with zero demagnetization factor, the formalism is capable of handling an arbitrary field dependence of $J_c(B)$. A realistic calculation encompassing samples with nonzero demagnetization factors would be extremely tedious and we conjecture that the classification of minor hysteresis loops presented is independent of the sample demagnetization factor.

[1]C. P. Bean, Rev. Mod. Phys. **36**, 31 (1964).
[2]L. Ji, H. Sohn, G. C. Spalding, C. J. Lobb, and M. Tinkham, Phys. Rev. B **40**, 10 936 (1989).
[3]K. H. Muller, J. C. Macfarlane, and R. Driver, Physica C **158**, 366 (1989).
[4]R. Novarro, F. Lera, C. Rillo, and J. Bartolome, Physica C **167**, 549 (1990).
[5]Q. H. Lam, Y. Kim, and C. D. Jeffries, Phys. Rev. B **42**, 4846 (1990).
[6]S. F. Wahid and N. K. Jaggi, Physica C **170**, 395 (1990).
[7]T. Ishida and R. B. Goldfarb, Phys. Rev. B **41**, 8937 (1990).
[8]A minor hysteresis loop is distinguished from the more commonly calculated magnetization hysteresis curve in that the latter has $B_{dc}=0$.
[9]M. A. R. LeBlanc, G. Fillion, and J. P. Lorrain, J. Appl. Phys. **59**, 3208 (1986).

[10]S. F. Wahid and N. K. Jaggi, Physica C **184**, 88 (1991).
[11]G. Ravi Kumar and P. Chaddah, Phys. Rev. B **39**, 4704 (1989).
[12]Y. Yeshurun, M. W. McElfresh, A. P. Malozemoff, J. Hagerhorst-Trewhella, J. Mannhart, F. Holtzberg, and G. V. Chandrashekhar, Phys. Rev. B **42**, 6322 (1990).
[13]K. V. Bhagwat and P. Chaddah, Phys. Rev. B **44**, 6950 (1991).
[14]Such a generalized field variable was also earlier used to calculate ac losses. See J. R. Clem, J. Appl. Phys. **50**, 3518 (1979).
[15]Shailendra Kumar, S. B. Roy, P. Chaddah, Ram Prasad, and N. C. Soni, Physica C **191**, 450 (1992).
[16]Shailendra Kumar, S. B. Roy, P. Chaddah, Ram Prasad, and N. C. Soni (unpublished).
[17]M. Xu, D. Shi, and R. F. Fox, Phys. Rev. B **42**, 10 773 (1990).
[18]R. B. Goldfarb, A. F. Clark, A. I. Braginski, and A. J. Panson, Cryogenics **27**, 475 (1987).
[19]P. Chaddah, G. Ravikumar, A. K. Grover, C. Radhakrishnamurty, and G. V. Subba Rao, Cryogenics **29**, 907 (1989).
[20]S. Senoussi, M. Oussena, M. Ribault, and G. Collin, Phys. Rev. B **36**, 4003 (1987).
[21]P. Chaddah, Pramana **36**, 353 (1991).